CHAPTER 2

Chapter 2

Instability of a vertical thermosyphon with nearly parallel branches

2.1. Introduction

A thermosyphon is a circulating fluid system whose motion is caused by density differences in a body force field which result from heat transfer. Thus, it is well to note that all systems to which the name thermosyphon has been applied in formal studies are in fact systems which have the intrinsic function of removing heat from a prescribed source and transporting heat and mass over a specific path (frequently a recirculating flow) and rejecting the heat or mass to a prescribed sink. That is, the path of the circulating flow which transports the thermal energy is or can be totally prescribed.

Free convection loops (thermosyphons), created by heating from below and cooling from above, have applications in geophysical processes and energy conversion systems. Natural convection flows in thermosyphons have long been attractive for technological applications. Hydrothermal circulations in the earths' crust have been observed in surface thermal springs on the continents (Waring (1965)) and as warm water vents on the ocean floor (Crane and Normark (1977), Corliss *et al* (1979)).

Closed loop thermosyphon is a very natural geometric configuration that can be found (or easily created) in many industrial situations. It

avoids the entry choking or mixing that occurs in the open thermosyphon. Thus, in addition to being convenient and common, the closed loop thermosyphon should be capable of attaining much larger heat transfer rates.

In principle there is virtually no limit to the types of flow that could be obtained in a closed loop subject to various thermal, geometric, body forces and thermodynamic state conditions. Most cases so far considered have been simple single-phase, continuous, loop flows.

Some of the previous studies of natural circulation loops were concerned with the stability of the steady-state motion, including the early analyses of Keller (1966) and Welander (1967). Zvirin *et al* (1978) studied the stability characteristics of the common thermosyphonic solar water heater and showed that this system can become unstable at high energy utilizations. Zvirin (1979) studied the effects of dissipation on the steady state and stability of thermosyphons. A theoretical method was presented by Zvirin (1985) for the study of the onset of motion in a symmetrical natural circulation loop consisting of two vertical parallel branches. He result showed that there exists a critical modified Rayleigh number, R_c, below which the rest state is stable and any flow perturbation will decay.

Asymmetric loops where heating is applied (even partly) from the side is encountered in energy conversion systems such as thermosyphonic

solar water heaters (Zvirin *et al* (1978)) and exergency core cooling of nuclear reactors (Zvirin (1981), Jeuck *et al* (1981), Zvirin and Y. Rabinovitz (1982), Y. Zvirin *et al* (1981)).

The present analysis deals with the instability associated with the onset of global flow around vertical loops with nearly parallel branches as shown in figure (2.1). The stability margin of the rest state is sought, which corresponds to the onset of a global motion around the loop. A one dimensional model is adopted, as in the previous studies because we are interested in the initial state of a disturbance in the form of a flow around the whole loop. The flow is assumed to be laminar and the fluid properties are considered to be constant except for the evaluation of the density in producing buoyancy. For this term alone, the density is assumed to vary linearly with temperature. Also we have taken into account the rate of dissipation of energy in the equation of heat conduction.

2.2. Mathematical formulation

Welander (1967) suggested that insight into the mechanism of convection in a finite region, being heated at the lower portion and cooled at the upper portion, can be obtained by considering a very simple model: A one-dimensional fluid moving along a given closed loop and subjected to given heat sources and sinks along its path. Such a model can be materialized by taking a narrow tube of uniform cross-section and

forming it into a closed loop. The loop is filled with fluid that is well-mixed over the cross-section.

Welanders' (1967) analysis was restricted to a simple model in which the tube consists of two vertical branches of length L/2 with connections at the top and bottom. The tube was taken to be symmetric with respect to the vertical.

We consider the vertical nearly-parallel loop consisting of one vertical and another inclined (at an angle δ measured in radians) insulated branches connecting two rigid containers. We are interested in the onset of global motion around the loop from the rest state. Thus the velocities developed are small and laminar flow prevails. We adopt the Boussinesq approximation where $\rho = \rho_0 [1 - \beta(T - T_0)]$. The equations governing the flow are given as follows

$$\nabla . \vec{q} = 0 \qquad (2.2.1)$$

$$\rho_0 \left[\frac{\partial \vec{q}}{\partial t} + (\vec{q} . \nabla) \vec{q} \right] = - \nabla p + \rho g + \mu \nabla^2 \vec{q} \qquad (2.2.2)$$

where ρ, g, μ, p, $\vec{q}$ denote density, acceleration due to gravity, co-efficient of viscosity, pressure, velocity of the fluid.

We make use of an one-dimensional model with V and T representing cross-sectional average velocity and temperature in the vertical branches. The single spatial co-ordinate s, runs around the loop.

The one dimensional continuity equation (2.2.1) indicates that the flow rate or the velocity of the circulating fluid is a function of the time only;

$$V = V(t) \tag{2.2.3}$$

Pressure can be eliminated from equation (2.2.2) by integrating around the loop.

$$\rho_0 \oint \frac{ds}{A} \frac{dQ}{dt} = - g \oint \rho \, dz - \oint f V^2 \frac{ds}{d_H} \tag{2.2.4}$$

where z is the vertical coordinate, A is the cross-sectional area, V is the velocity and Q = AV, f is the friction factor and d_H is the hydraulic diameter of the flow channel.

For simplicity we take the vertical branches to be circular pipes with radius a. In this study we shall limit ourselves to the cases in which the viscous effects become less important and can therefore be replaced by an approximation. Hence the frictional force is assumed to be proportional to the velocity. We thus have $\nu \nabla^2 V = - C V$ where the friction factor, for laminar flow in these pipes is roughly equal to 16/Re = 16v / 2aV following Zvirin (1979, 1985), Re is Reynolds number. It is assumed that the pipes are long enough so that the pressure drops in the connections to the containers are negligible and are wide enough so that the effect of surface tension is vanishingly small.

Equation (2.2.4) can be rewritten as

$$\rho_0 \left[\int \frac{dz}{A}\frac{dV}{dt} A + \int \frac{dz}{A}\frac{dV}{dt} A \sec\delta\right]$$

$$= -g\rho_0 \int [1-\beta(T_r - T_l)]\, dz$$

$$-\frac{\rho_0}{a}\left[\int f V^2\, dz + \int f V^2 \sec\delta\, dz\right]$$

from which we obtain

$$\frac{dV}{dt} = \frac{\beta g}{h(1-\sec\delta)} \int (T_r - T_l)\, dz - \frac{8\nu V}{a^2} \qquad (2.2.5)$$

where h is the height of the loop and the subscripts r and l denote the right and left branches and δ is the angle of inclination of the left branch to vertical. In obtaining equation (2.2.5) f is replaced by 16/Re. The energy equation for the insulated pipes is

$$\frac{\partial T}{\partial t} + (V.\nabla)\, T = \alpha \nabla^2 T + \Phi \qquad (2.2.6)$$

where α is the thermal diffusivity and Φ is the rate at which energy is dissipated by viscosity in each element of volume of the fluid. Φ in equation (2.2.6), following Zvirin (1979), is expressed as V^2 with a constant multiplier ϕ. Hence for the right and left branches, the equation (2.2.6) will assume the following form

$$\frac{\partial T}{\partial t} + V\frac{\partial T}{\partial z} = \alpha \frac{\partial^2 T}{\partial z^2} + \phi V^2 \qquad \text{for the right branch}$$

$$\frac{\partial T}{\partial t} - V\cos\delta\, \frac{\partial T}{\partial z} = \alpha \frac{\partial^2 T}{\partial z^2}\cos^2\delta + \phi V^2$$

for the left branch

(2.2.7)

In order to solve the partial differential equations (2.2.7) boundary conditions must be specified. For the completely closed loop these are replaced by the requirement that the temperature is continuous around the loop.

We prescribe the following boundary conditions for the temperature determined by the containers :

$$T_r = T_l = T_D \qquad \text{at } z = 0$$

$$T_r = T_l = T_U \qquad \text{at } z = h \tag{2.2.8}$$

In order to compare theoretical and experimental results of various loops,. a presentation based on non-dimensional parameters should be adopted. To transform the equations (2.2.5) - (2.2.8) into the non-dimensional form, we let h, $V_{ch} = \beta\, g\, (T_D - T_U)\, a^2 / 16\nu$, h/V_{ch}, $\theta = (T - T_U)/(T_D - T_U)$ to characterize the length, velocity, time and temperature respectively. The replacement of the variables $\vec{r}$, $\vec{q}$, t, T by their scaled counter parts allows reduction of the problem to the following dimensionless form

$$\frac{\partial V}{\partial t} = \int_0^1 (\theta_r - \theta_l)\, dz - V \tag{2.2.9}$$

$$P \frac{\partial \theta}{\partial t} + RV \frac{\partial \theta}{\partial z} = \frac{\partial^2 \theta}{\partial z^2} + R\, \phi\, V^2 \qquad \text{for right branch}$$

$$P \frac{\partial \theta}{\partial t} - RV \cos\delta \frac{\partial \theta}{\partial z} = \cos^2\delta \frac{\partial^2 \theta}{\partial z^2} + R\, \phi\, V^2 \quad \text{for left branch} \tag{2.2.10}$$

and the boundary conditions are

$$\theta_r = \theta_l = 1 \qquad \text{at } z = 0$$

$$\theta_r = \theta_l = 0 \qquad \text{at } z = 1 \tag{2.2.11}$$

where the parameter P and R are modified Prandtl and Rayleigh numbers, defined by

$$P \equiv 8 \left(\frac{h}{a}\right)^2 \frac{\nu}{\alpha} = 8 \left(\frac{h}{a}\right)^2 Pr ;$$

$$R = \frac{V_{ch} h}{\alpha} = \frac{\beta g}{16 \alpha \nu} (T_D - T_U)\, a^2 h \tag{2.2.12}$$

2.3. Analysis of steady state solutions

Most of the existing studies on natural circulation loops are concerned with stability of steady state motion. The steady state motion in natural circulation loops is dominated by the dimensionless parameter R, modified Rayleigh number and the loop geometry. At steady state all the time dependent terms disappear and equations (2.2.9) - (2.2.11) can be rewritten as

$$V = \int_0^1 (\theta_r - \theta_l)\, dz \tag{2.3.1}$$

$$RV \frac{\partial \theta}{\partial z} = \frac{\partial^2 \theta}{\partial z^2} + R\phi V^2$$

$$- RV \cos\delta \frac{\partial \theta}{\partial z} = \cos^2\delta \frac{\partial^2 \theta}{\partial z^2} + R\phi V^2 \tag{2.3.2}$$

and $\theta_r = \theta_l = 1$ at $z = 0$

$$\theta_r = \theta_l = 0 \qquad \text{at } z = 1 \tag{2.3.3}$$

The steady state velocity V is constant around the loop. The energy equation (2.3.2) is therefore solved for θ with V as a parameter.

The solution is written in the following form

$$\theta_r = C_1 + C_2 e^{RVz} + V\phi z + \frac{\phi}{R}$$

$$\theta_l = C_3 + C_4 e^{-RV\eta z} - V\phi\eta z + \frac{\phi}{R} \tag{2.3.4}$$

where η is the secant of the angle of inclination of the left branch i.e. $\eta = \sec \delta$.

Introducing the temperature distribution (2.3.4) with boundary conditions (2.3.3) the following relations are obtained for the constants of integration C_i

$$C_1 = \frac{e^{RV} + V\phi}{e^{RV} - 1} - \frac{\phi}{R} \qquad C_2 = \frac{1 + V\phi}{1 - e^{RV}}$$

$$C_3 = \frac{e^{-RV\eta} + V\phi\eta}{e^{-RV\eta} - 1} - \frac{\phi}{R} \quad C_4 = \frac{1 - V\phi\eta}{1 - e^{-RV\eta}} \tag{2.3.5}$$

The temperature distributions (2.3.4) with (2.3.5) are introduced now with the momentum equation (2.3.1). Evaluating the temperature integrals we obtain by letting w = RV,

$$\frac{\frac{w}{R}\phi(1+\eta)(e^{w(1-\eta)} - 1) + (\frac{w}{R}\phi(1-\eta) + 2)(e^{-w\eta} - e^{w})}{2(e^{-w\eta} - 1)(e^{w} - 1)}$$

$$- \frac{1}{w}(1 + \frac{1}{\eta}) - \frac{w}{R} = 0 \tag{2.3.6}$$

which is a non-linear algebraic equation for the velocity w depending on the parameter R. This equation has been solved numerically and the steady state velocity is plotted as a function of Rayleigh number in figures (2.2) - (2.5).

We are mainly interested in the onset of instability when the velocities are small. Therefore we seek a solution for w << 1. Expanding the equation (2.3.6) asymptotically for very small velocities, we obtain

$$w = \frac{\phi(1-\eta^2) \pm \sqrt{\phi^2(1-\eta^2)^2 + 2(12 - R(1+\eta))[\phi\eta(1-\eta)^2 + \frac{1}{30}(1+\eta^3)]}}{\phi\eta(1-\eta)^2 + \frac{1}{30}(1+\eta^3)} \qquad (2.3.7)$$

This leads to the smallest Rayleigh number for which there is steady flow as

$$R_c = \frac{12}{1+\eta} + \frac{\phi^2(1-\eta^2)^2}{2(1+\eta)[\phi\eta(1-\eta)^2 + \frac{1}{30}(1+\eta^3)]} \qquad (2.3.8)$$

For Rayleigh number smaller than R_c we have no steady flow.

From equation (2.3.8) it may be noted immediately that for a nearly parallel loop, dissipation has no effect on the critical Rayleigh number. The critical value R_c for which the steady flow exists is decreased due to the inclination of the branches. Also when the loop is vertical with parallel branches i.e., $\eta = 1$, the dissipation has no effect on the critical Rayleigh number and steady state velocity, which confirms the result obtained by Zvirin (1979).

2.4. The onset of motion

2.4.1. Stability of the equilibrium state

It is shown in the previous section that no steady flow can be established in the loop when the modified Rayleigh number, R is below a critical value R_c. Now, we aim at analysing the stability characteristics associated with the onset of motion in the loop. The basic technique is linear stability analysis, in which the effect of a small fluctuation away from a solution to the equations is examined as a function of the parameter R, the modified Rayleigh number. The analysis is in terms of normal modes of the system which constitute a complete set of eigenfunctions of the problem.

By supposing that the various physical variables describing the flow suffer small (infinitesimal) increments, we first obtain the equations governing these increments. We therefore write the time independent velocity and temperature as the steady values with superimposed perturbations :

$$V = \overline{V} + V e^{\sigma t} \; ; \quad \theta = \overline{\theta} + \psi e^{\sigma t} \tag{2.4.1}$$

where σ is the stability parameter.

Substituting equation (2.4.1) in the momentum and energy equations, we obtain the governing equations of the perturbed state as

$$V\ (\sigma + 1) \quad = \quad \int_0^1 (\psi_r - \psi_l)\ dz \tag{2.4.2}$$

$$\frac{\partial^2 \psi_r}{\partial z^2} - w \frac{\partial \psi_r}{\partial z} - P\ \sigma\ \psi_r - RV \frac{\partial \bar{\theta}_r}{\partial z} + 2\ w\ \phi\ V \quad = \quad 0 \tag{2.4.3}$$

$$\frac{\partial^2 \psi_l}{\partial z^2} - w\ \eta \frac{\partial \psi_l}{\partial z} - P\ \sigma\ \eta^2 \psi_r + RV\ \eta \frac{\partial \bar{\theta}_l}{\partial z} + 2\ w\ \phi V^2 \quad = \quad 0 \tag{2.4.4}$$

together with the boundary conditions

$$\psi_r \quad = \quad \psi_l \quad = \quad 0 \qquad \text{at } z = 0,\ 1 \tag{2.4.5}$$

where the non-dimensional steady state velocity is given by $\bar{V} = w/R$.

In obtaining these equations from the relevant equations of motion, we neglect all products and powers (higher than the first) of the increments and retain only terms which are linear in them. The linearized equations are to be solved to determine whether the fluctuations decay or grow in time.

Solving equations (2.4.3) and (2.4.4), we obtain

$$\psi_r \quad = \quad A_1\ e^{m_1 z} + A_2 e^{m_2 z} + \frac{Vw}{P\sigma} \left[\phi + (R + \phi\ w) \frac{e^{wz}}{e^w - 1} \right]$$

$$\psi_l \quad = \quad A_3\ e^{-m_1 \eta z} + A_4 e^{-m_2 \eta z}$$

$$+ \frac{Vw}{P\sigma} \left[\phi + (R - \phi\ \eta w) \frac{e^{-\eta wz}}{e^{-w\eta} - 1} \right] \tag{2.4.6}$$

where the arbitrary constants A_i's are determined by using equation (2.4.5), as follows

$$A_1 = \frac{Vw}{P\sigma}\left[\phi\,\frac{(e^{m_2}-1)}{e^{m_1}-e^{m_2}} + (R+\phi w)\,\frac{e^{m_2}-e^{w}}{(e^{m_1}-e^{m_2})\,(e^{w}-1)}\right]$$

$$A_2 = \frac{Vw}{P\sigma}\left[\phi\,\frac{(1-e^{m_1})}{e^{m_1}-e^{m_2}} + (R+\phi w)\,\frac{e^{w}-e^{m_1}}{(e^{m_1}-e^{m_2})\,(e^{w}-1)}\right]$$

$$A_3 = \frac{Vw}{P\sigma}\left[\phi\,\frac{(e^{-m_2\eta}-1)}{e^{-m_1\eta}-e^{-m_2\eta}} + (R-\phi w\,\eta)\,\frac{e^{-m_2\eta}-e^{-w\eta}}{(e^{-m_1\eta}-e^{-m_2\eta})\,(e^{-w\eta}-1)}\right].$$

$$A_4 = \frac{Vw}{P\sigma}\left[\phi\,\frac{(1-e^{-m_1\eta})}{e^{-m_1\eta}-e^{-m_2\eta}} + (R-\phi w\,\eta)\,\frac{e^{-w\eta}-e^{-m_1\eta}}{(e^{-m_1\eta}-e^{-m_2\eta})\,(e^{-w\eta}-1)}\right] \qquad (2.4.7)$$

where

$$m_{1,2} = \frac{w \pm \sqrt{w^2+4P\sigma}}{2}$$

Introducing equation (2.4.6) into equation (2.4.2) and evaluating the integral, we obtain the characteristic equation for the stability parameter as

$$\frac{P\sigma(\sigma+1)}{w} = \frac{R}{w}\left(1+\frac{1}{\eta}\right) + \phi\,\frac{(e^{m_1}-1)\,(e^{m_2}-1)}{e^{m_1}-e^{m_2}}\left(\frac{1}{m_1}-\frac{1}{m_2}\right)$$

$$+ \phi\,\frac{(e^{-m_1\eta}-1)\,(e^{-m_2\eta}-1)}{e^{-m_1\eta}-e^{-m_2\eta}}\left(\frac{1}{m_1}-\frac{1}{m_2}\right)\frac{1}{\eta}$$

$$+ (R+\phi w)\,\frac{1}{e^{m_1}-e^{m_2}}\;\frac{1}{e^{w}-1}$$

$$\{\frac{(e^{m_1}-1)\ (e^{m_2}-e^{w})}{m_1}+\frac{(e^{m_2}-1)\ (e^{w}-e^{m_1})}{m_2}\}$$

$$+(R-\phi w\eta)\ \frac{1}{e^{-m_1\eta}-e^{-m_2\eta}}\ \frac{1}{e^{-w\eta}-1}$$

$$\{\frac{(e^{-m_1\eta}-1)\ (e^{-m_2\eta}-e^{-w\eta})}{m_1\eta}$$

$$+\frac{(e^{-m_2\eta}-1)\ (e^{-w\eta}-e^{-m_1\eta})}{m_2\eta}\}$$

(2.4.8)

2.4.2. Stability of rest state

We now consider the stability of the rest state. The rest state is governed by equations (2.2.9) - (2.2.11) with $\overline{V} = 0$. The exact solution in this case is,

$$\overline{\theta}_r = \overline{\theta}_l = 1 - z$$

which obviously satisfies the momentum equation (2.2.9), in that there is no net buoyancy force, due to symmetry.

The perturbed equations (2.4.2) - (2.4.4) yield

$$\int_0^1 (\psi_r - \psi_l)\ dz = V(\sigma + 1) \qquad (2.4.9)$$

$$\frac{\partial^2 \psi_r}{\partial z^2} - P\sigma\psi_r = -RV \qquad (2.4.10)$$

$$\frac{\partial^2 \psi_l}{\partial z^2} - P\sigma\psi_l \eta^2 = RV\eta \qquad (2.4.11)$$

The boundary conditions are same as in equation (2.4.5)

The eigenfunctions ψ_r and ψ_I are given by

$$\psi_r = A_1 e^{\lambda z} + A_2 e^{-\lambda z} + \frac{RV}{P\sigma} \tag{2.4.12}$$

$$\psi_I = A_3 e^{\eta\lambda z} + A_4 e^{-\lambda\eta z} - \frac{RV}{P\sigma} \tag{2.4.13}$$

where $\lambda^2 = P\,\sigma$

$$A_1 = \frac{RV}{P\sigma}\,\frac{e^{-\lambda}-1}{e^{\lambda}-e^{-\lambda}}$$

$$A_2 = \frac{RV}{P\sigma}\,\frac{1-e^{\lambda}}{e^{\lambda}-e^{-\lambda}}$$

$$A_3 = -\frac{RV}{P\sigma}\,\frac{e^{-\lambda\eta}-1}{e^{\lambda\eta}-e^{-\lambda\eta}}$$

$$A_4 = -\frac{RV}{P\sigma}\,\frac{1-e^{\lambda\eta}}{e^{\lambda\eta}-e^{-\lambda\eta}} \tag{2.4.14}$$

Making use of ψ_r and ψ_I, from equations (2.4.12) - (2.4.14) in equation (2.4.9), the characteristic equation for the stability parameter σ is obtained as

$$P\,\sigma\,(\sigma+1) = 2R\left[1 - \frac{e^{\lambda}-1}{\lambda\,(e^{\lambda}+1)} - \frac{(e^{\lambda\eta}-1)}{\lambda\,\eta\,(e^{\lambda\eta}+1)}\right] \tag{2.4.15}$$

It is observed from equation (2.4.15) that the dissipation parameter does not influence the stability of the rest state.

Expanding the above equation in the neighbourhood of $R = R_c$, we obtain a double solution for λ, with $\lambda << 1$, given by

$$\lambda = \pm \left[\frac{R(1+\eta^2) - 12}{\frac{12}{P} + \frac{R}{10}(1+\eta^4)} \right]^{1/2} \qquad (2.4.16)$$

Introducing $R = \frac{12}{1+\eta}$ in the denominator of the last relationship, we obtain

$$\lambda = \pm \left[\frac{R(1+\eta^2) - 12}{\frac{12}{P} + \frac{6}{5}\frac{(1+\eta^4)}{1+\eta}} \right]^{1/2} \qquad (2.4.17)$$

When $R > \frac{12}{1+\eta^2}$, there are two real roots for λ, and from the relation $\lambda^2 = P\sigma$ we find the following single value for σ;

$$\sigma = \frac{R(1+\eta^2) - 12}{12 + \frac{6P}{5}\frac{(1+\eta^4)}{1+\eta}} > 0 \qquad (2.4.18)$$

For $R < \frac{12}{1+\eta^2}$, equation (2.4.17) yields a double imaginary solution for λ which leads to the following single solution for σ.

$$\sigma = - \left[\frac{12 - R(1+\eta^2)}{12 + \frac{6P}{5}\frac{(1+\eta^4)}{1+\eta}} \right] < 0 \qquad (2.4.19)$$

From equations (2.4.18) and (2.4.19) we find that for all values of modified Prandtl number we obtain a single eigenvalue σ, near the critical modified Rayleigh number. Thus, σ is positive and the rest state is unstable when $R > \frac{12}{1+\eta^2}$ and σ is negative and the rest state is stable when $R < \frac{12}{1+\eta^2}$.

2.5. Numerical results

From the experimenters' point of view, thermal convection is a particularly simple subject of research because of the absence of a mean flow.

The particular choice of the dimensionless parameters of the problem offers the advantage that the onset of convection depends only on the Rayleigh number. The Prandtl number measures the relative importance of the advection of momentum and heat.

Restricting the attention to convection in a finite region, we find that fluid particle carries out a periodic or quasiperiodic motion between the top and the bottom, being heated at the lower portion and cooled at the upper portion of its orbit. To obtain insight into the mechanism of such a convection, in the previous section we have considered an one dimensional fluid moving along a given closed loop.

The stability associated with the onset of motion in a toroidal thermosyphon has been investigated by two methods a) derivation of a steady state solution for the flow in the loop and determination of the condition for its existence b) direct stability analysis of the equilibrium state. The results show that there exists a critical value of the modified Rayleigh number which depends on the angle of inclination of the left branch to the right branch.

We have solved equation (2.3.6) for steady state velocity as a function of the modified Rayleigh number R. Curves representing steady state velocity w are presented in figures (2.2) - (2.5). In these figures, we may observe that, for large R, w varies linearly with R which is to be expected, as it can be seen from equation (2.3.6) that for large R, the expression becomes w = R– 2. From figures (2.2) - (2.5), it may be deduced that steady state velocity w increases with R, ϕ and η. In figure (2.5) it is illustrated that dissipation does not have any effect on the steady state velocity when η = 1. This result is in agreement with the result obtained by Zvirin (1979).

In figures (2.6) and (2.7), we have illustrated the behaviour of the stability parameter σ when the constant steady state velocity is w. A numerical investigation of characteristic equation (2.4.8) reveals that it always has a real root for $R > \frac{12}{1+\eta^2}$. When the angle of inclination of the left branch of the loop is zero, we see that the equation (2.4.8) has a real root for R > 6 which was originally obtained by Zvirin (1985). Thus the critical Rayleigh number decreases for decreasing values of η. Hence we deduce that when the thermosyphon is modelled so as to have mutually inclined branches, the range of the values of Rayleigh number, for which the existence of steady flow is possible, becomes wider.

In figures (2.6) - (2.8), (2.12), (2.13) we have illustrated the growth rate σ as a function of Rayleigh number for P = 0.1, 1.0, 10.0,

100.0, for a fixed η = 1.0 and 2.0 when ϕ = 0.1, 0.5 and 0.0. Equation (2.4.8) has always a real negative root which corresponds to stable mode. For very small Rayleigh number, the growth rate decreases very rapidly and approaches a constant value for higher Rayleigh numbers as compared to the case η = 1. We find from figures (2.6) - (2.8) that increase in the Prandtl number results in the increase of the growth rate of perturbation. We may also note that, the increment in σ is very small, even though the Prandtl number is increased considerably.

To clearly understand the effect of dissipation ϕ on an inclined thermosyphon, we have plotted the growth rate σ of perturbations in figure (2.9) as a function of ϕ for η = 2.0 and P =1.0. We may conclude from figure (2.9) that increase in ϕ decreases the growth rate σ of perturbations.

When the Prandtl number and co-efficient of dissipation are kept constant, it is seen from figures (2.10) and (2.11) that the rate of decay of the disturbance decreases for increasing angle of inclination.

Comparing figures (2.9) and (2.14) we see that the stability parameter σ changes significantly with dissipation factor ϕ when $\eta \neq 1$ but it is independent of ϕ when η = 1, for given values of R, which is the affirmation of the result obtained by Zvirin (1979).

From figures (2.6) - (2.14) it is observed that an inclined thermosyphon with a constant steady state velocity w is stable when dissipation is included.

In figures (2.15) - (2.18), we have depicted the behaviour of stability parameter σ as a function of R when the steady state velocity is zero. It may be observed from figures (2.15) and (2.16) that there exists a monotonous mode of perturbation growth with a rate which increases with increase in R and decreases as P increases when η is fixed.

It can be elucidated from figures (2.17) and (2.18) that when the Prandtl number is constant, stability parameter decreases with decreasing η.

From figures (2.15) - (2.18) it may be concluded that the rest state of the thermosyphon is always unstable. In figure (2.16), we have reproduced the case $\eta = 0$ of Zvirin (1985). From equation (2.4.15) it is observed that the stability of the rest state of a thermosyphon with non-parallel branches is unaffected by dissipation as in the case of vertical parallel branch thermosyphon.

2.5. Conclusion

We have considered the stability associated with the onset of motion in one-dimensional vertical loop when the two branches of the thermosyphons are nearly parallel. Boussinesq approximation is employed and normal mode approach to linear stability has been adopted. We have

found the critical value of the Rayleigh number. For $R > R_c$, the rest state of the loop is always unstable. It is found that high angle of inclination decreases the stability of the natural convection loop. Also an inclined thermosyphon with a constant steady state velocity $w \neq 0$ is stable. Stability parameter σ decreases with dissipation. Dissipation does not affect steady state flow rate of a vertical thermosyphon and the stability characteristics of the rest state of an inclined thermosyphon.

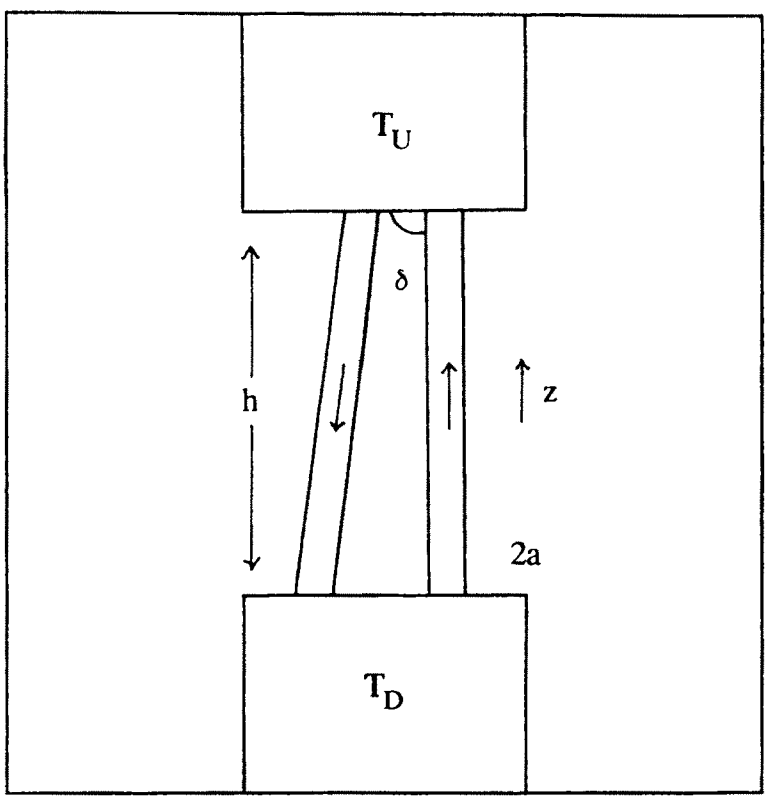

Fig. 2.1. An illustration of vertical thermosyphon with nearly parallel branches

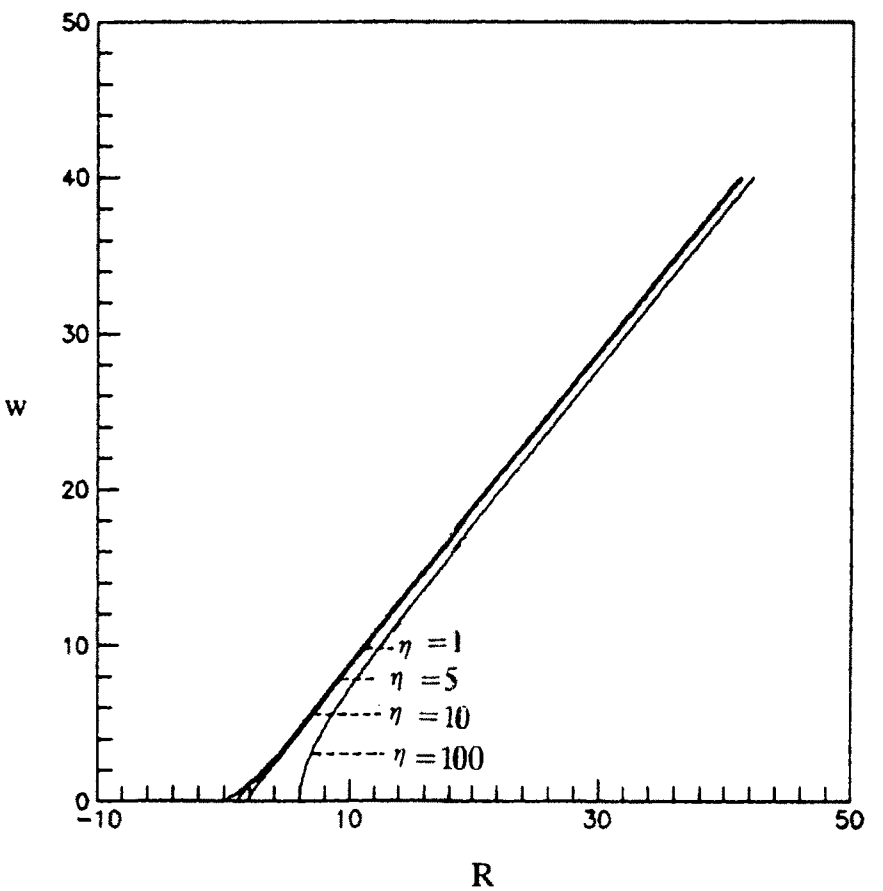

Fig. 2.2. Variation of steady state velocity w as a function of Rayleigh number R for various η ($\phi = 0$)

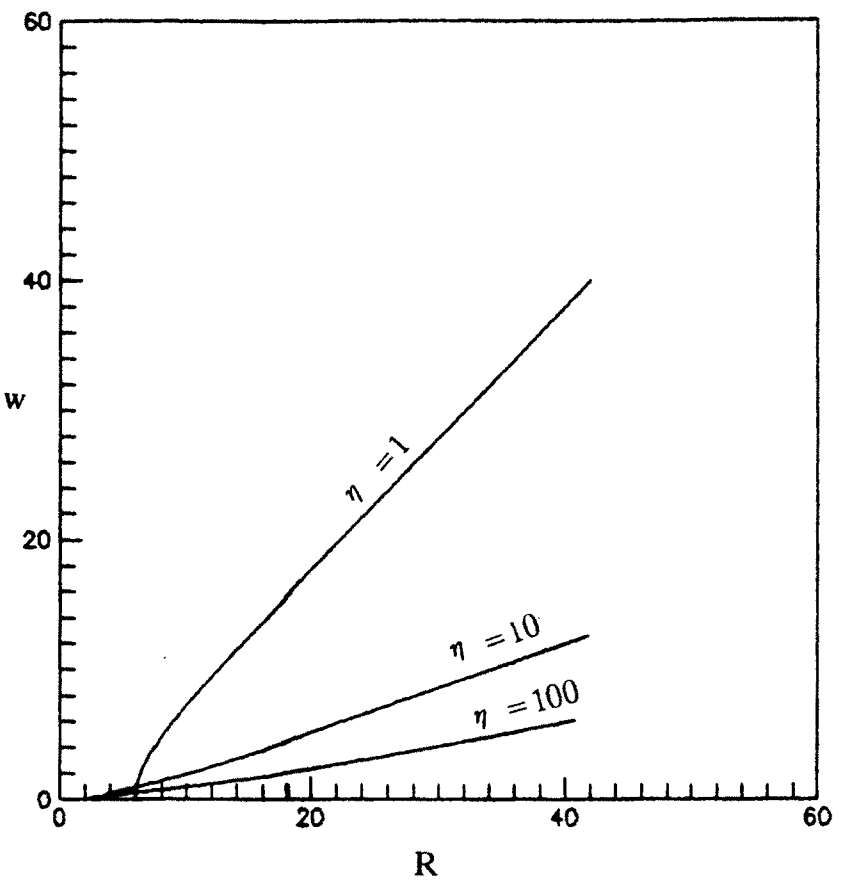

Fig. 2.3. Variation of steady state velocity w as a function of R for $\phi = 1$

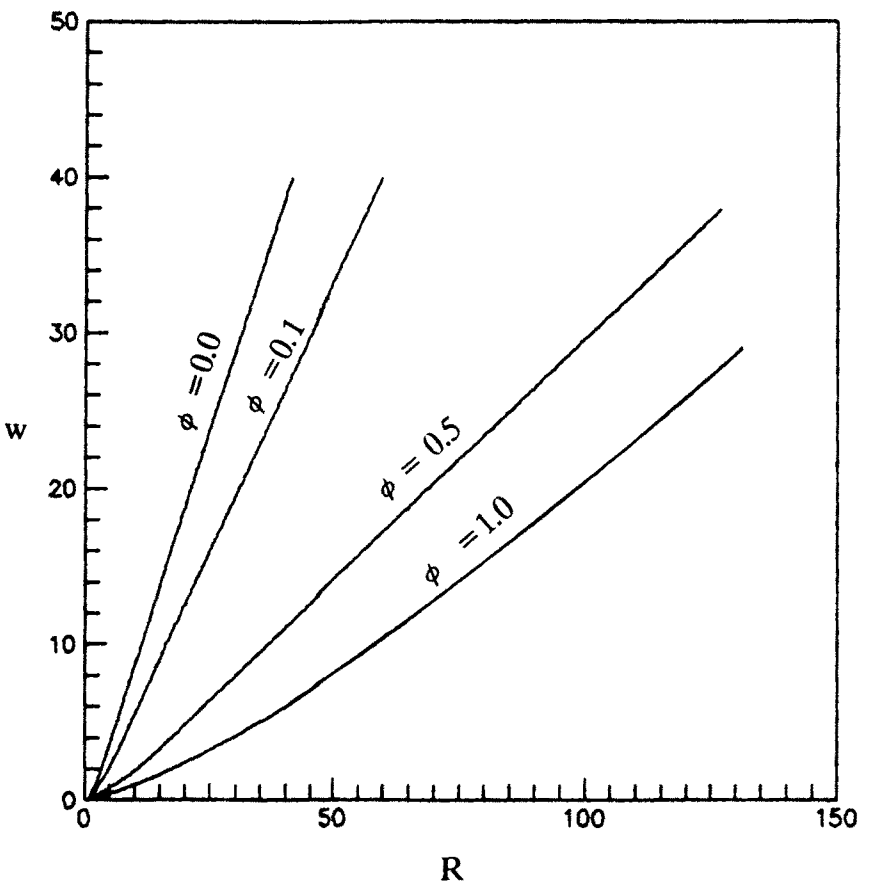

Fig. 2.4. Variation of steady state velocity w with respect to R for various dissipation parameter with $\eta = 10$

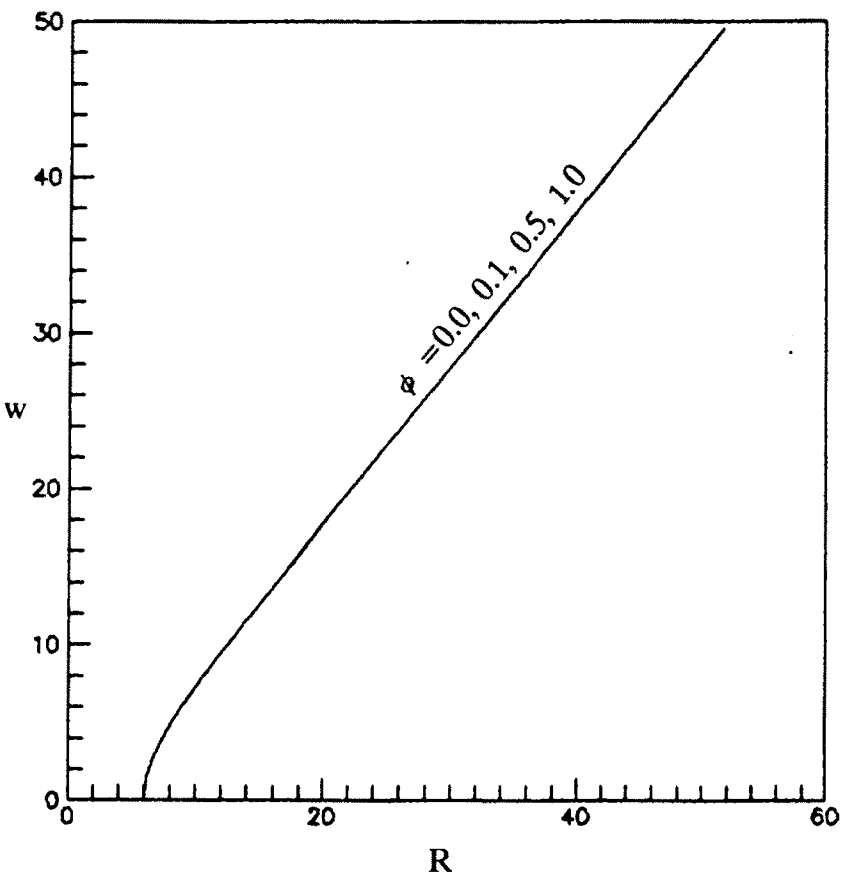

Fig. 2.5. Variation of w with respect to R for $\eta = 1$

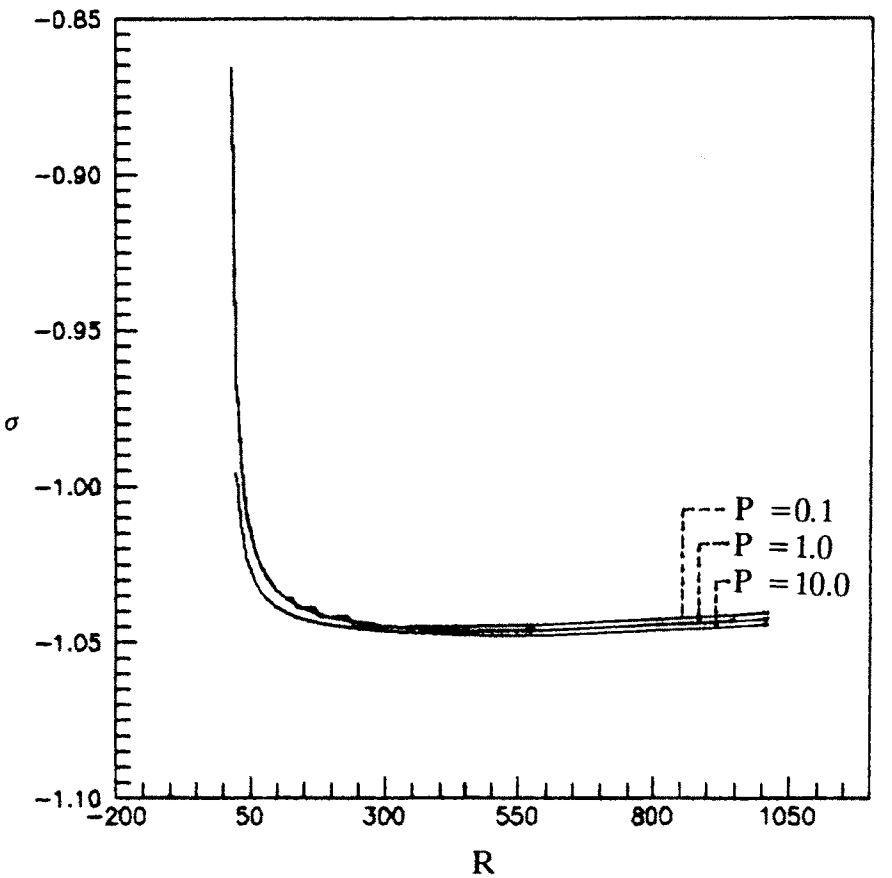

Fig. 2.6. Dependence of σ on R for fixed $\eta = 2$ $\phi = 0.1$ (w is constant)

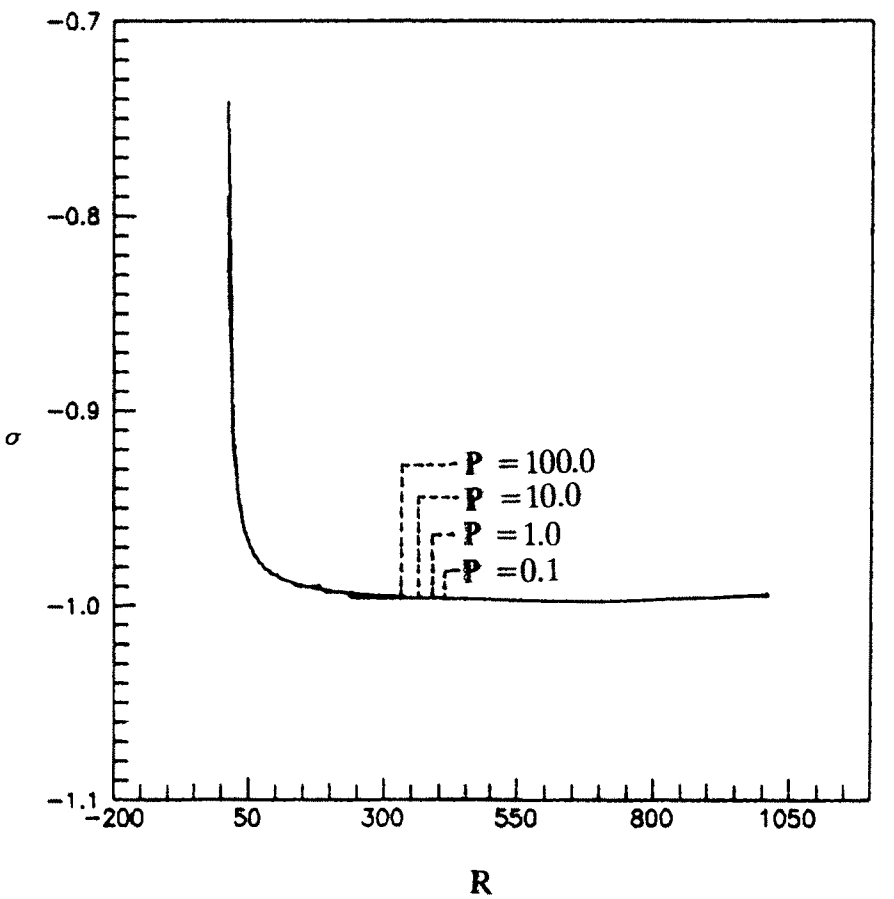

Fig. 2.7. Dependence of σ on R for $\eta = 2., \phi = 0$ (w is constant)

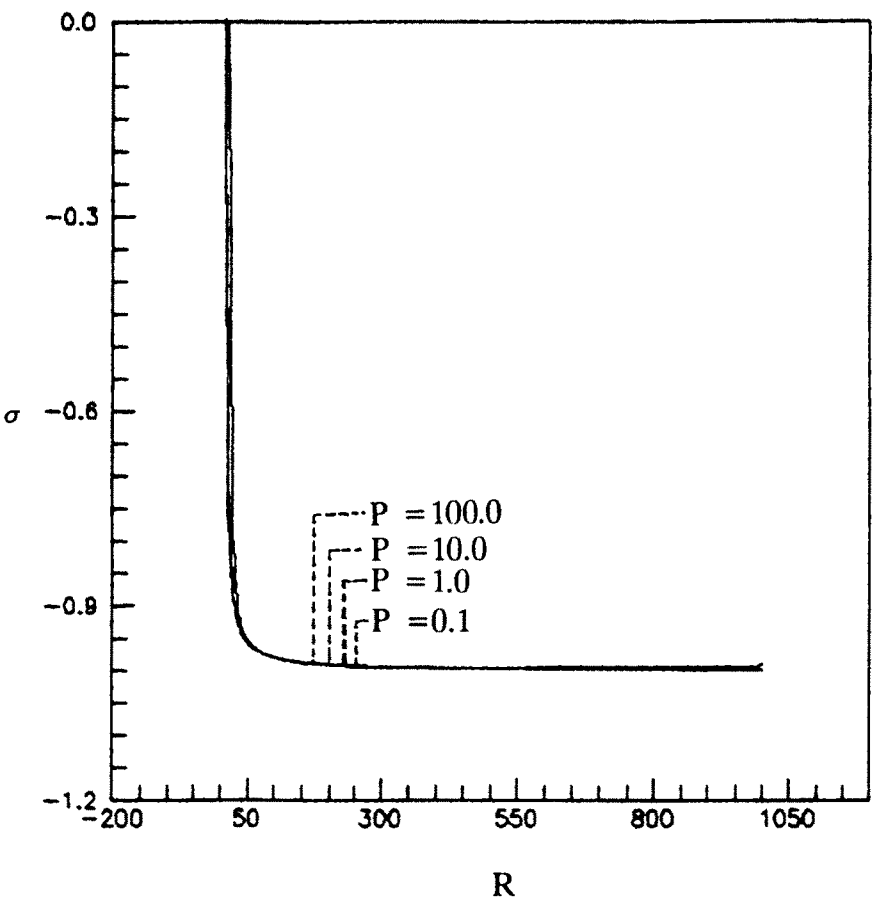

Fig. 2.8. Dependence of σ on R for η =1.0 ϕ =0.5 (w is constant)

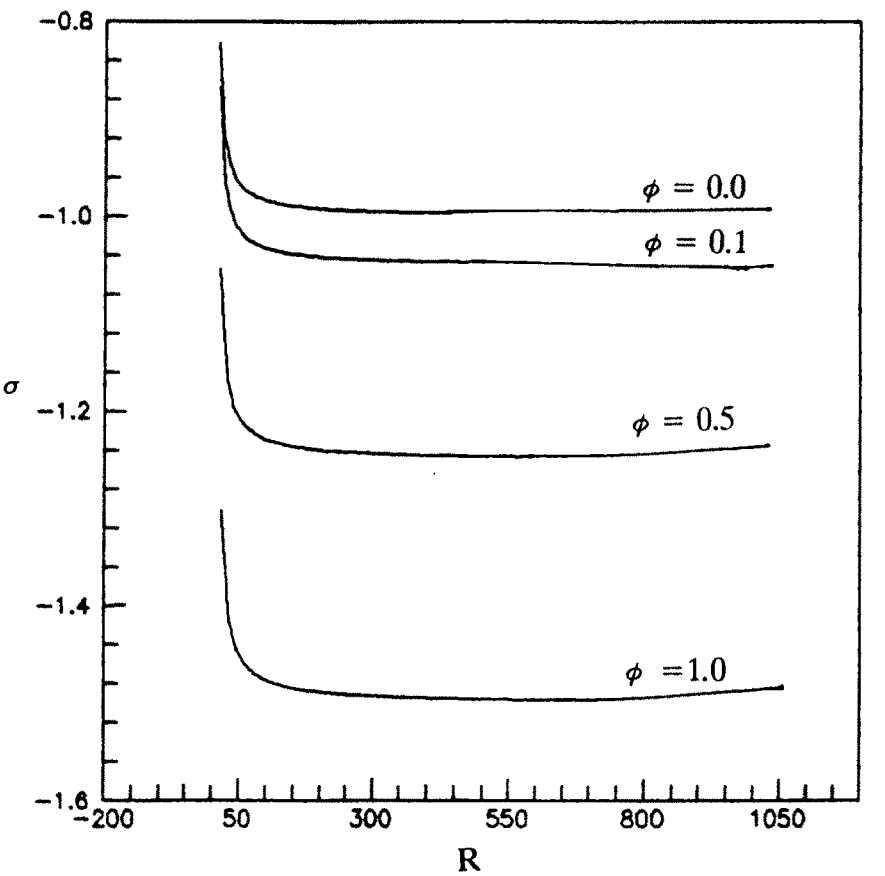

Fig. 2.9. Dependence of σ on R for $\eta = 2$, P = 1.0 (w is constant)

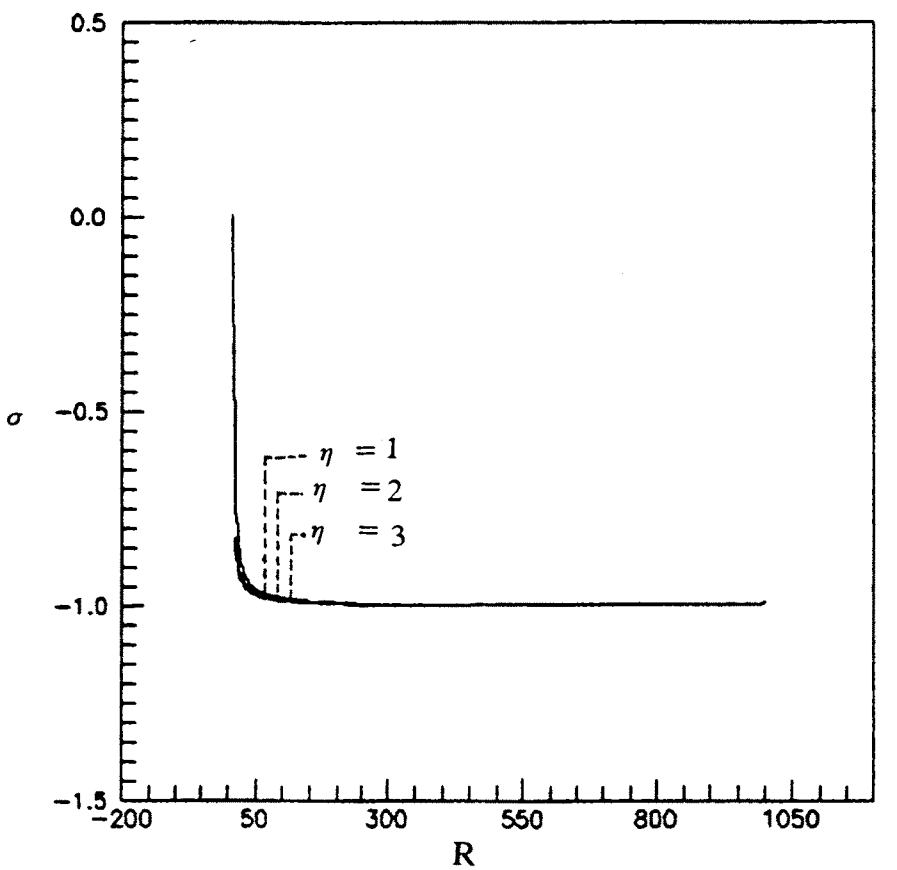

Fig. 2.10. Decay rate σ vs. R for ϕ = 0.0, P = 1.0 (w is constant)

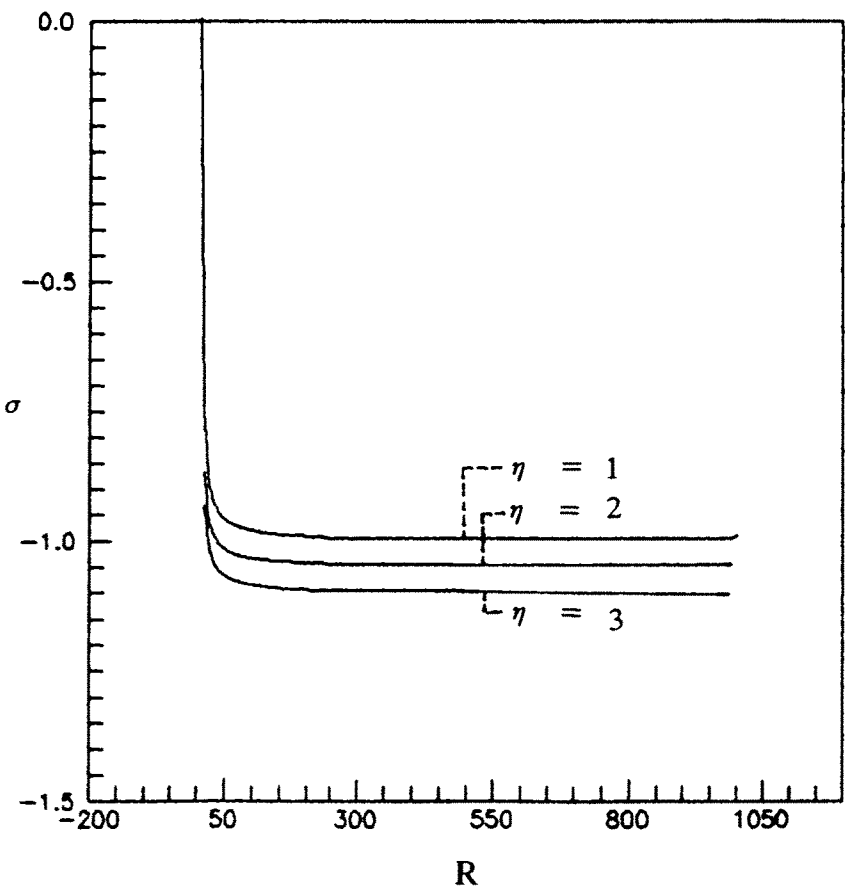

Fig. 2.11. Decay rate σ vs. R for ϕ =0.1 P =0.1
(w is constant)

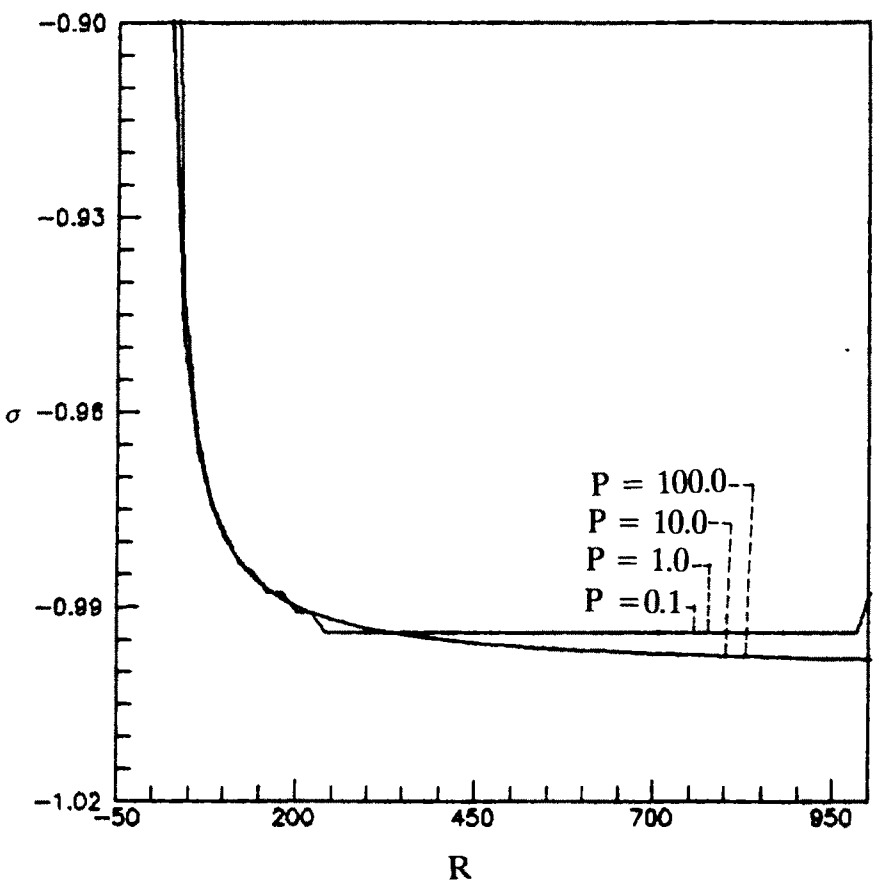

Fig. 2.12. Decay rate σ vs. R for various values of P, $\eta = 1.0, \phi = 0.0$

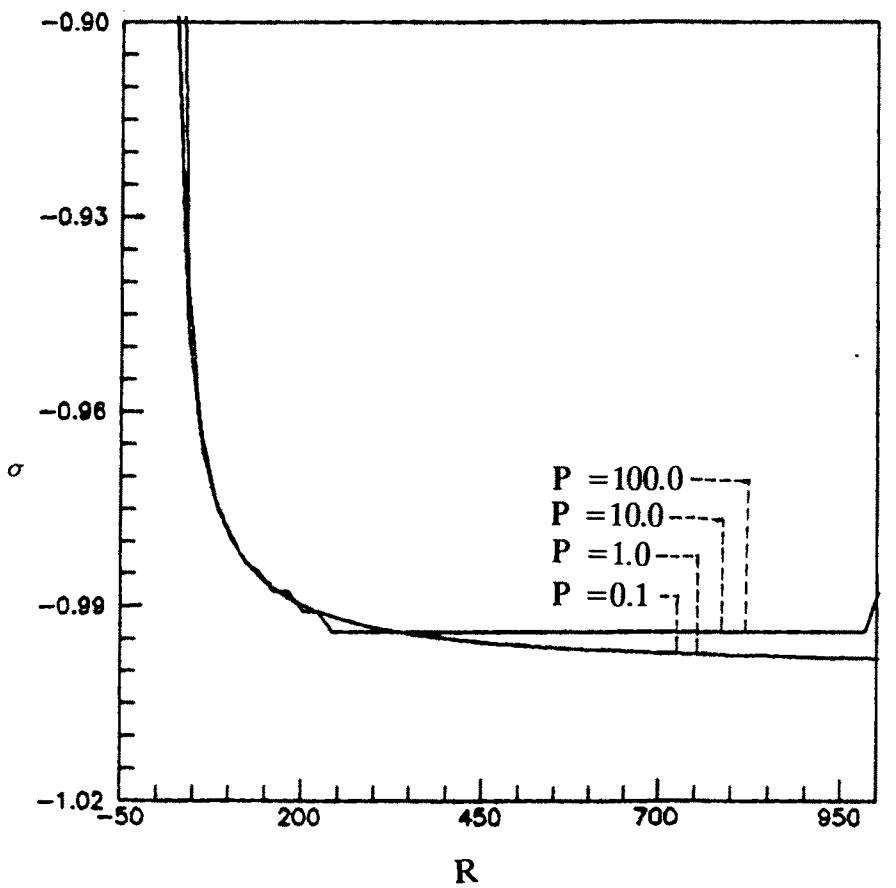

Fig. 2.13. Growth rate σ for various values of P

$\eta = 1.0, \phi = 1.0$

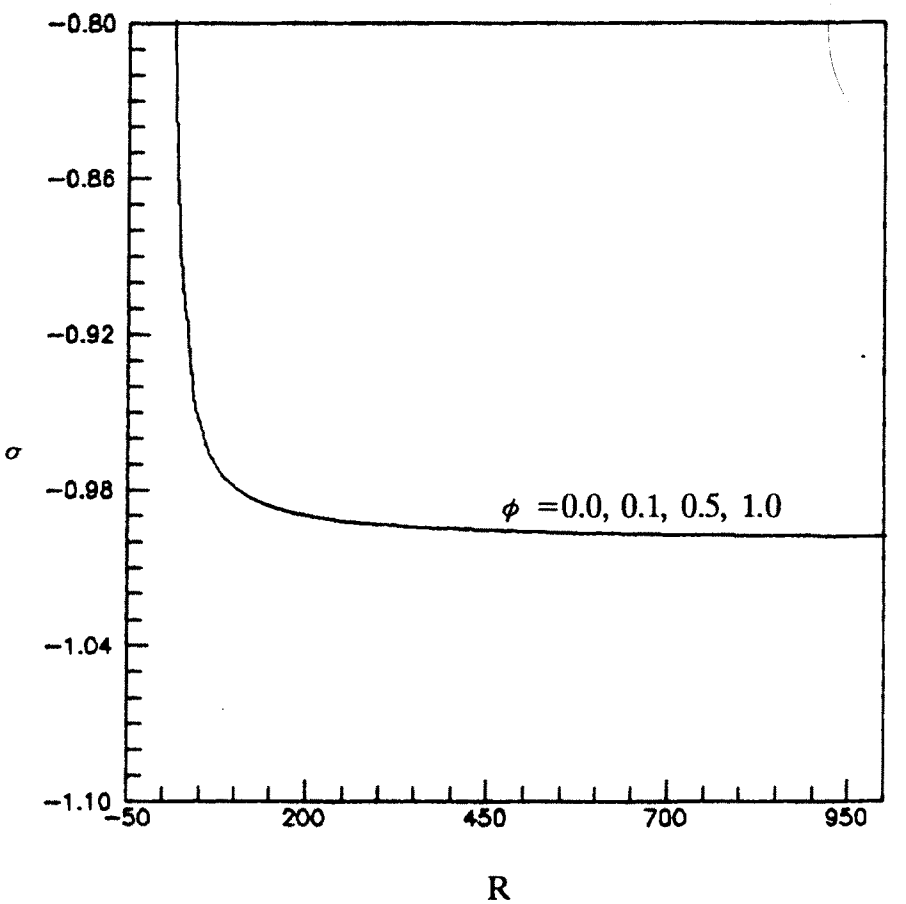

Fig. 2.14. Growth rate σ for various values of ϕ

$\eta = 1.0$, P = 1.0

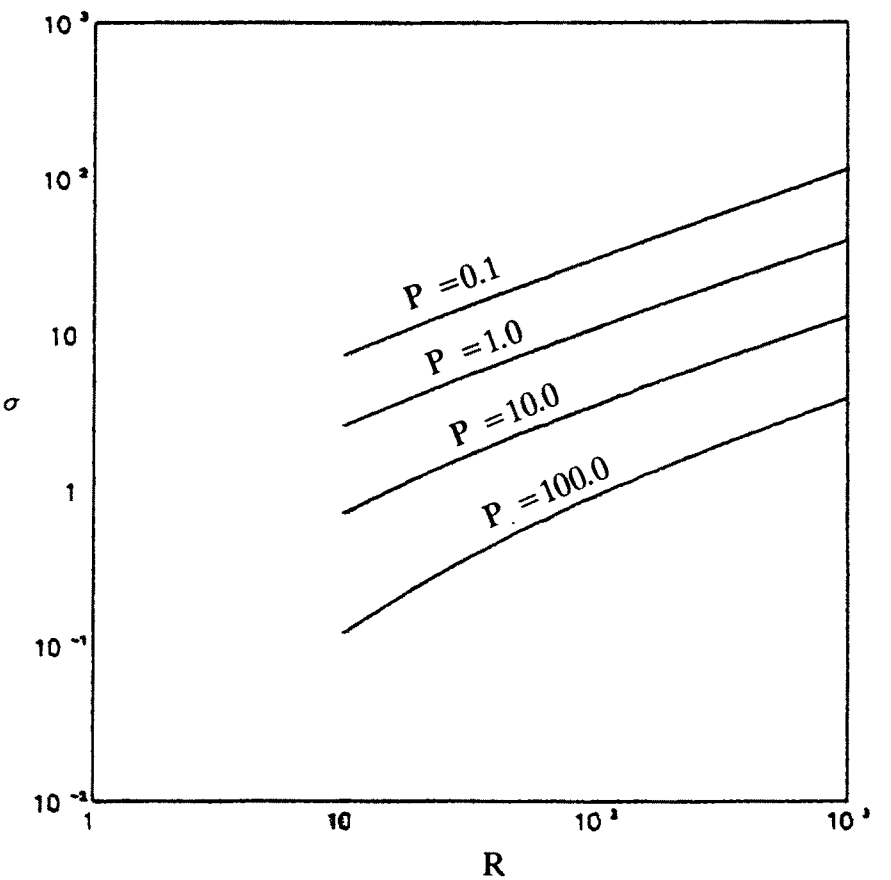

Fig. 2.15. Growth rate σ of the steady state disturbance versus **R** for different P (w = 0, η = 5)

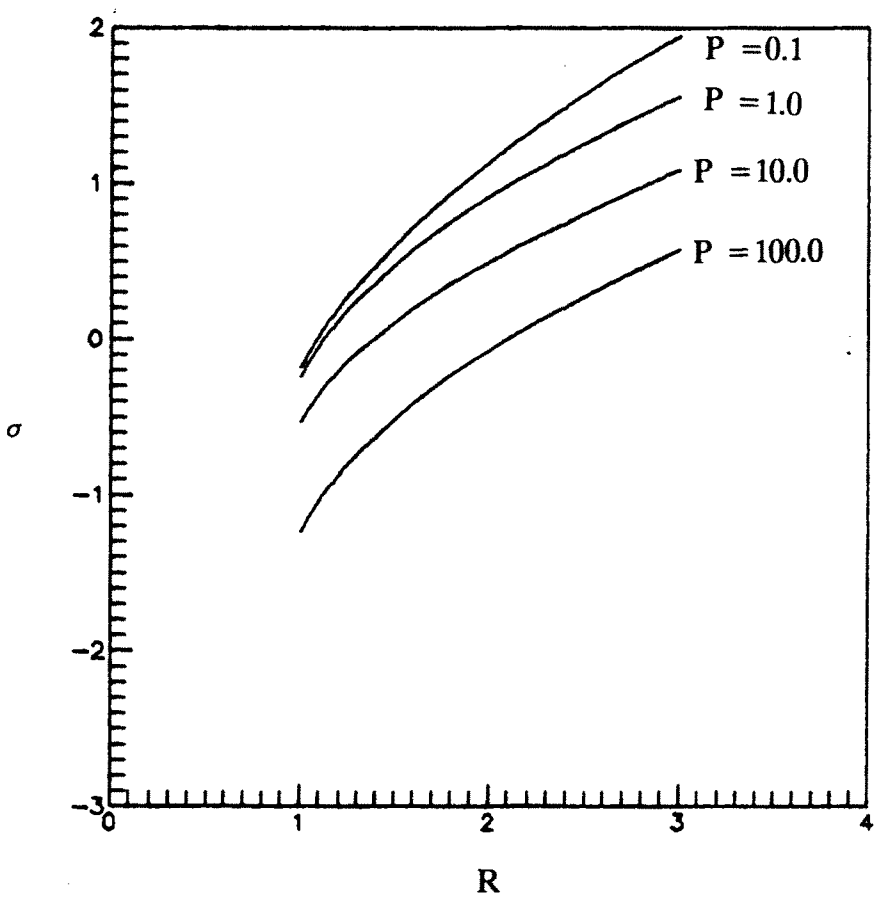

Fig. 2.16. Growth rate σ of the steady state disturbance versus R for different P (w = 0, σ = 1.0)

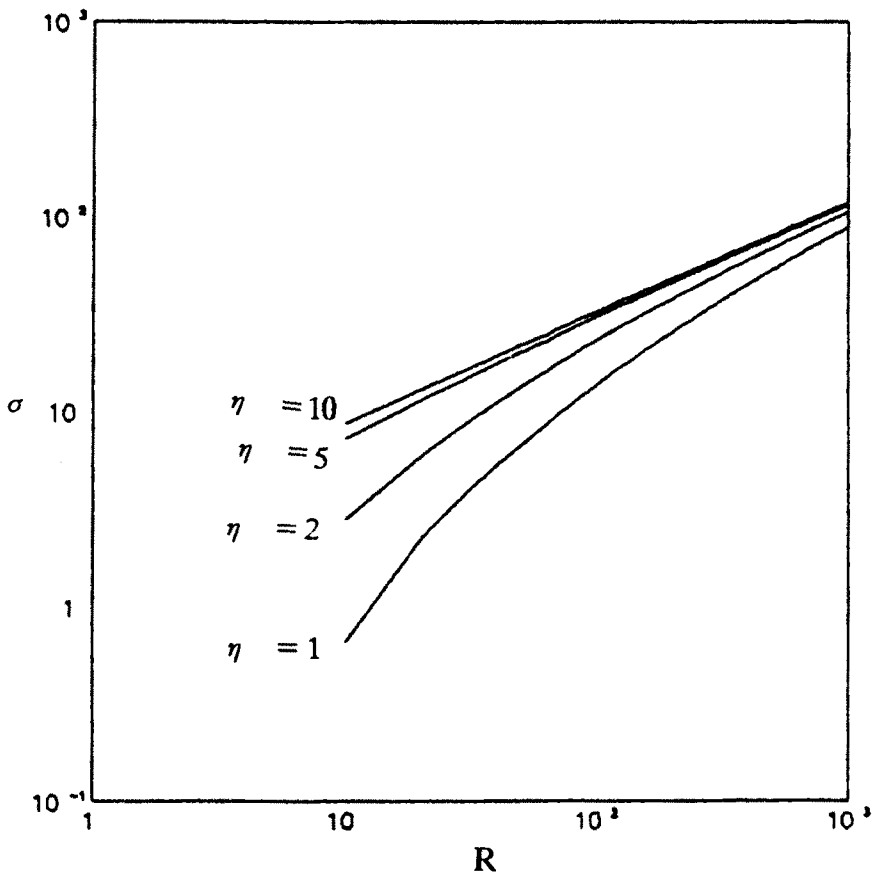

Fig. 2.17. Growth rate σ as a function of R for various values of σ (P =0.1)

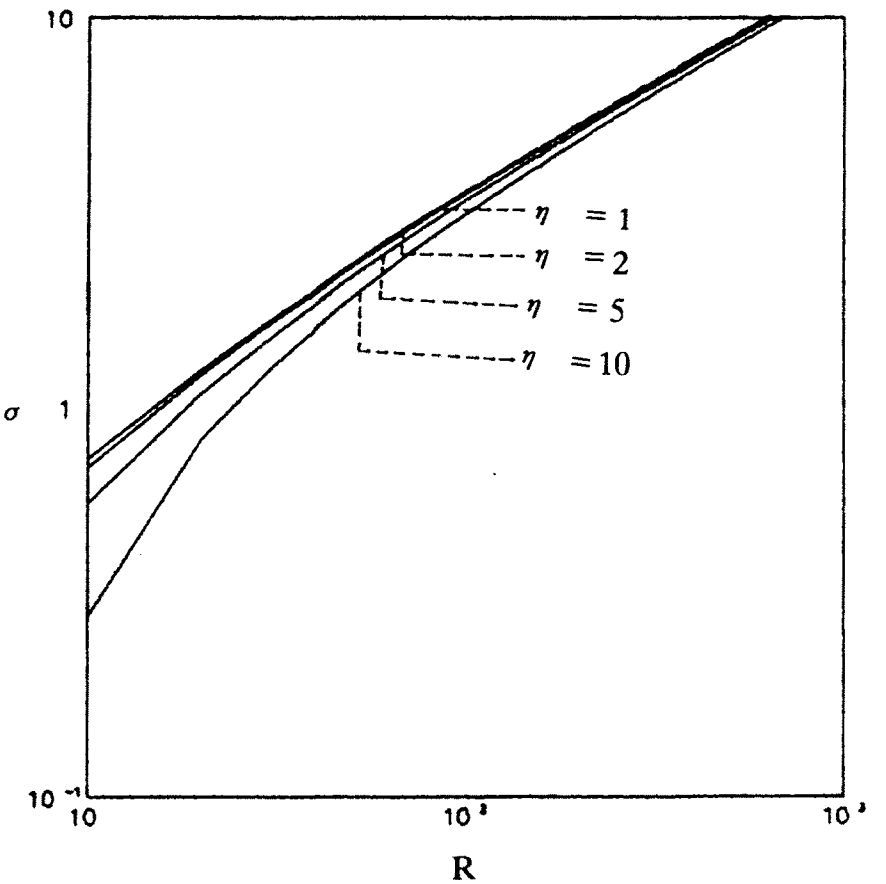

Fig. 2.18. Growth rate σ as a function of R for various values of σ (P =10.0)